Alzheimer's Disease "non-amyloidogenic" p3 peptide revisited: a case for Amyloid-α

Ariel J. Kuhn[a], Benjamin S. Abrams[b], Stella Knowlton[a], Jevgenij A. Raskatov[a]*

[a] Dept. of Chemistry and Biochemistry, University of California Santa Cruz, CA 95064, United States

[b] Dept. of Biomolecular Engineering, Life Sciences Microscopy Center, University of California Santa Cruz, CA 95064, United States

SUPPORTING INFORMATION

Table of Contents

General Experimental Procedures

Peptide Preparation. Purification of Aβ40 was done as previously published.[2] For p3, solid, lyophilized peptide was dissolved in 8:2 0.1% NH_4OH H_2O/acetonitrile and purified using PLRP-S columns (8 µm, 300 Å) under basic conditions. All peptide purities range from 95-99%. The concentration of p3 was determined by the absorbance of the peptide backbone at 205 nm via Nanodrop (ε = 83,370 M^{-1} cm^{-1}) using the protein parameter calculator (http://nickanthis.com/tools/a205.html).[3] The concentration of Aβ40 was determined at 280 nm (ε = 1490 M^{-1} cm^{-1}).

Microscopy. Samples were imaged on a JEOL 1230 microscope at University of California Santa Cruz or a Tecnai-12 microscope at University of California Berkeley.

Oligomer Image Analysis. The TEM images of oligomers were converted to 8-bit and the following filters were applied: 1) process → filters → median → radius = 4. 2) Image → Adjust → Auto Local Threshold → method = Phansalkar; radius = 15. 3) Process → Noise → Despeckle. 4) Process → Binary → Fill holes. 5) Process → Binary → Watershed. 6) Analyze → Set Measurements → Select Area, Limit to Threshold, Decimal places = 2. 7) Analyze → Analyze Particles → Set Size = 120 – infinity, Circularity = 0.35-1 → Add to Manager. The area values were then converted to diameters and displayed as a histogram.

ThT Assay. ThT (Acros Organics, 2390-54-7) was dissolved in 10 mL of PBS buffer containing 0.02% (w/v) NaN_3 and filtered through a 0.22 µm filter. The concentration was determined by Nanodrop at 412 nm (ε = 36000$M^{-1}cm^{-1}$). Lyophilized samples of peptide were prepared as described above at 20 µM, with 20 µM ThT in PBS. 200 µL of sample was added to each well, in triplicate, of a black, clear bottom 96-well plate. Absorbance readings were measured ever 5 min with 5 s of shaking before reading and 295 s of shaking between readings at 37 °C with a Biotek synergy HTX fluorescence plate reader (λ_{ex} = 444 nm λ_{em} = 485 nm).

TAMRA Quenching Assay. Lyophilized TAMRA-Aβ40 and TAMRA-p3 were each dissolved in 20 mM NaOH, and sonicated for 30 s. The samples were diluted in PBS and the corresponding concentrations were determined by Nanodrop (ε = 99000 M^{-1} cm^{-1}) at 555 nm. Readings were collected on a plate reader as described above (λ_{ex} = 550 nm λ_{em} = 580 nm).

Peptide structure images. Coordinates of peptide structures were downloaded from the pdb database (2M4J, 4NTR, 6CG4, and 3MOQ) and rendered using the freely available VMD software. Centroid-to-centroid distances were calculated using the ChemCraft program package.

Cellular viability. Lyophilized peptides were dissolved in 15 µL of 20 mM NaOH and the solutions were diluted to a final concentration of 50 µM with culture media. The samples were then incubated at 4 °C for 6 hours (consistent with method employed in Fig. 3 and S11, per published method by Ahmed *et. al.*[5]) The culture media intended for the vehicle cells as well as the blank samples was also incubated at 4 °C for 6 hours to account for any effects induced by low temperature. Human neuroblastoma SH-SY5Y cells were cultured in 1:1 DMEM: F12 K media supplemented with 10% fetal bovine serum and 1% penicillin-streptomycin. Cells were incubated at 37 °C with 5% CO_2. SH-SY5Y cells were plated in a 96-well plate at a density of 50,000 cells/well (100 µL total volume/well) and allowed to adhere for 24 h before dosing. After dosing, SH-SY5Y cells were incubated for 72 h at 37 °C. Then, 10 µL aliquots of WST-1 (Roche) were added to each well and incubated for 4 h. Then, absorbance was measured at λ = 490nm. Each bar represents an average of four replicates, normalized against the vehicle (cells and media only).

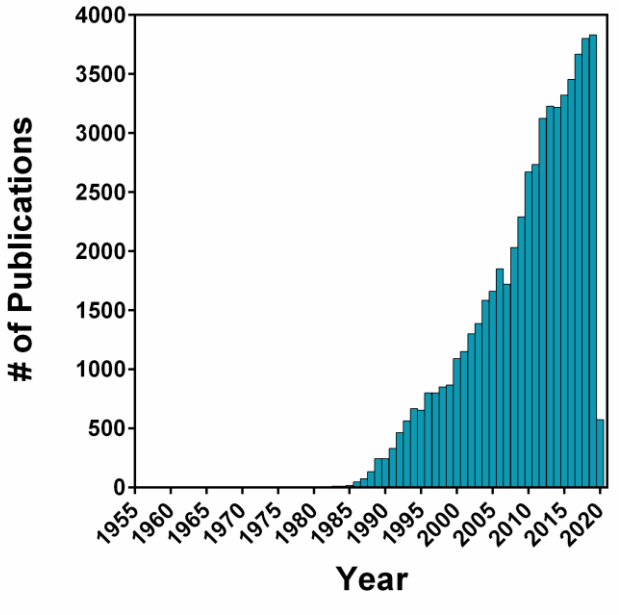

Figure S1. Histogram revealing number of annual publications on Aβ from 1955 until February 2020, according to PubMed.

Table S1. Literature analysis of conflicting findings characterizing the p3 peptide

CATEGORY	QUESTION	EVIDENCE TO SUPPORT	EVIDENCE TO CONTRADICT	AMBIGUOUS EVIDENCE
ISOLATION FROM AD PATIENTS	**From brains?**	1. p3 identified as major constituent of Down syndrome cerebellar preamyloid plaques[6] 2. major component of diffuse amyloid plaques[7]	1. No p3 isolated from sporadic AD brains[8]	1. p3 minor component of AD plaques[9] 2. p3 found in diffuse plaques and dystrophic neurites, but not in plaque cores[10]
	From cerebrospinal fluid (CSF)?	1. p3 levels in CSF correlates with mild cognitive impairment[11]		
AGGREGATION PROPENSITY	**Fibrilization possible?**	1. p3 formed irregular fibers[12] 2. fibril formation[13] 3. short fragments dissimilar to Aβ[14]	1. p3 formed intricate, dense lattices, unlike Aβ[15] 2. amorphous aggregates[6] 3. Small, granular particles[16]	1. Few p3 fibrils formed that were in dense networks shorter and narrower than Aβ[17]
	Theoretical simulations of fibrils	1. MD simulation of p3 fibrils[18]		
	ThT binding?	1. ThT positive[14,17]	1. ThT negative[15]	1. Very little ThT binding[6,12]
	Oligomerization possible?		1. Unable to trap oligomers[19]	
	Theoretical simulation of oligomerization	1. Molecular model of $A\beta_{18-41}$ oligomers[20] 2. MD simulations of theorized trimers and paranuclei[21] 3. MD simulations of theorized U- and S-shaped intermediates[22,23]	1. Simulations of p3 oligomers unstable[19]	
TOXICITY	**To cellular models?**	1. fresh and aged p3 found to be toxic to rat hippocampal neurons[17] 2. aged p3 toxic to SH-SY5Y cells[24] 3. toxicity to SH-SY5Y and IMR-32 cells[25] 3.p3 **formed** ion channels in cells, disrupting Ca^{2+} regulation, causing neuronal death[26] 4. p3 activated JNK and caspase-8[25]		
LONG-TERM POTENTIATION (LTP)	**Affected by p3?**		1. p3 found to not inhibit rat hippocampal LTP (11.5nM)[27]	
PRO-INFLAMMATORY CYTOKINE AND CHEMOKINE PRODUCTION	**Affected by p3?**	1. p3 stimulated production of IL-1α, IL-1β, IL-6, TNFα, MCP-1[28]		

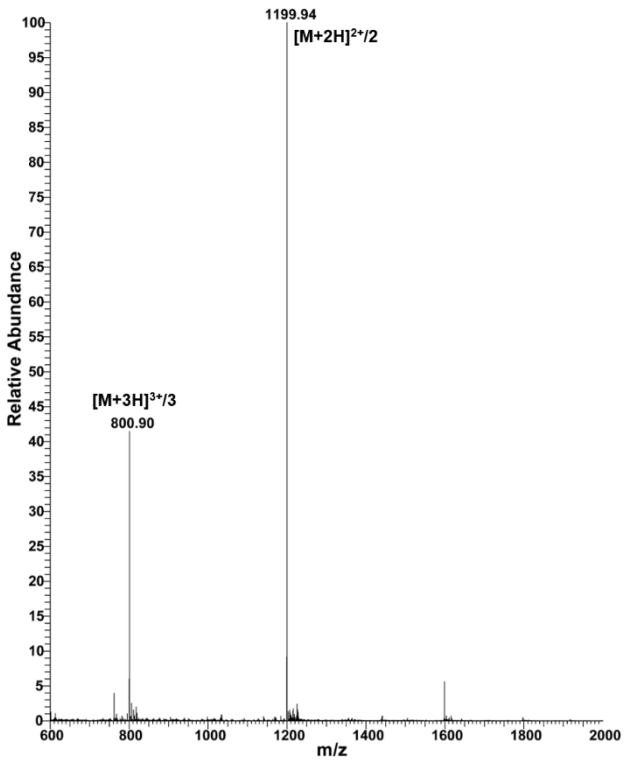

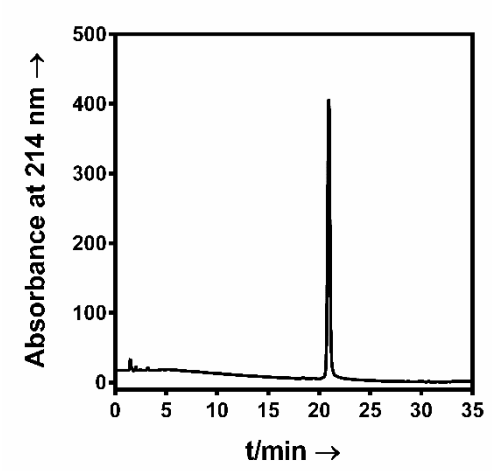

Peak #	Time (min)	Area	% Area
1	18.426	25.8	0.370
2	19.486	24.2	0.348
3	20.513	33.3	0.479
4	20.937	6876.5	98.803

Figure S2. Mass spectrometry and analytical HPLC characterization of a representative synthetic batch of $p3_{17\text{-}40}$.

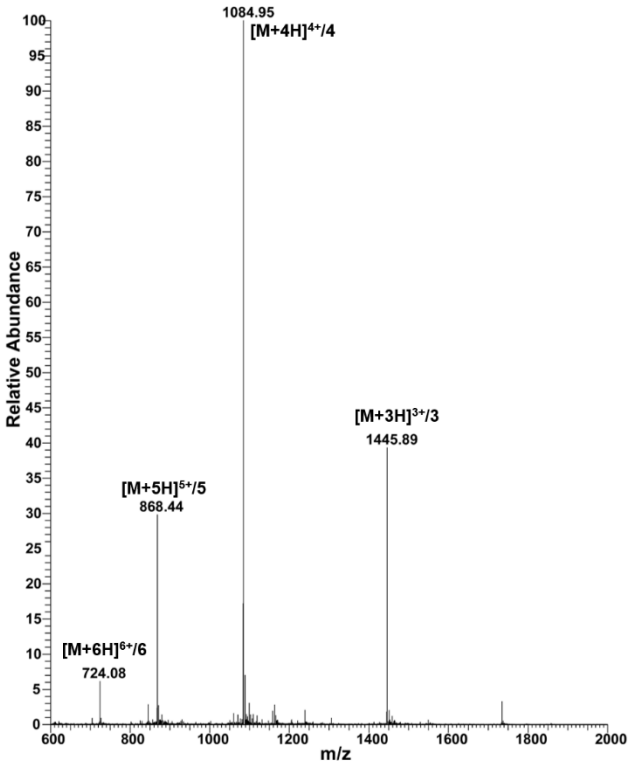

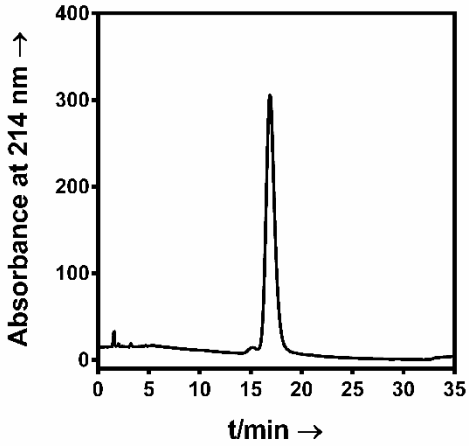

Peak #	Time (min)	Area	% Area
1	15.193	375.3	2.018
2	16.895	18187	97.786
3	19.121	36.4	0.196

Figure S3. Mass spectrometry and analytical HPLC characterization of a representative synthetic batch of $A\beta_{1\text{-}40}$.

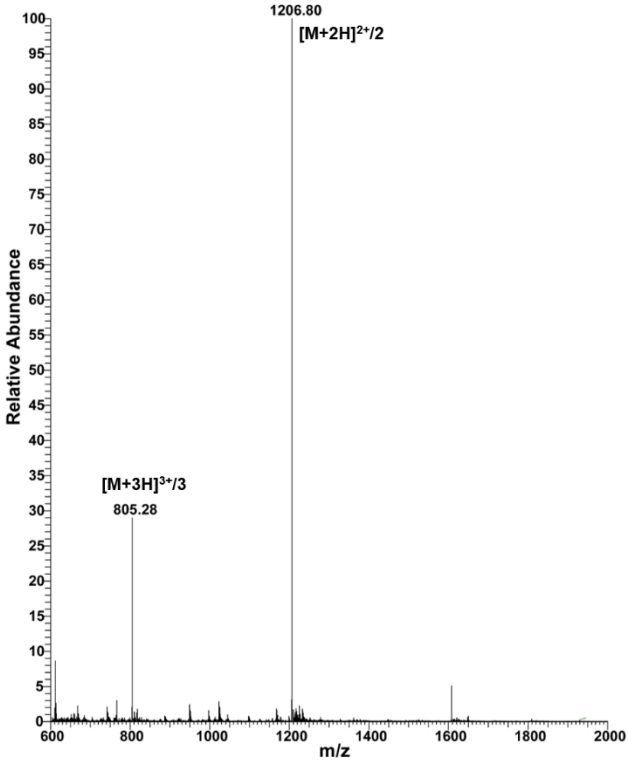

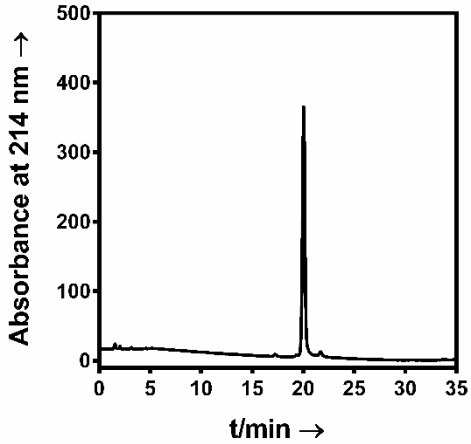

Peak #	Time (min)	Area	% Area
1	16.88	37.4	0.518
2	19.467	7210.8	98.672
3	20.972	59.2	0.810

Figure S4. Mass spectrometry and analytical HPLC characterization of a representative synthetic batch of $p3_{F19}$

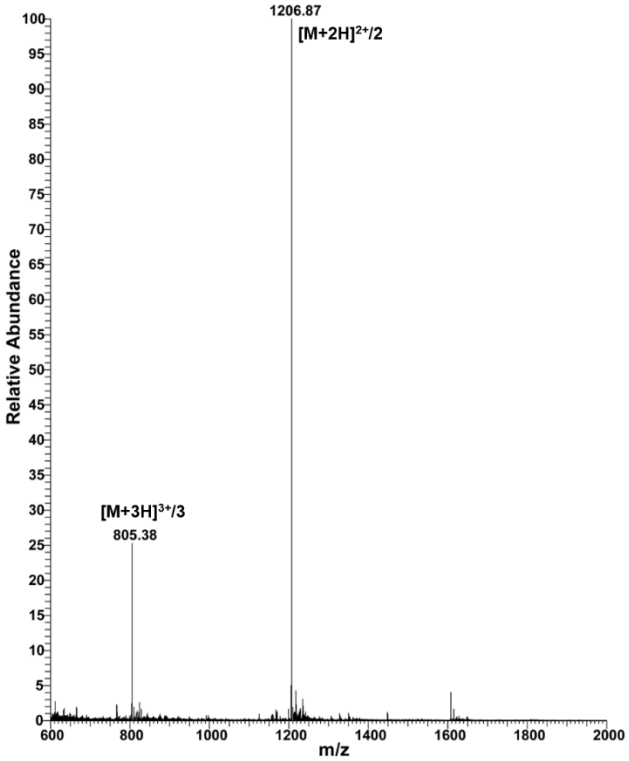

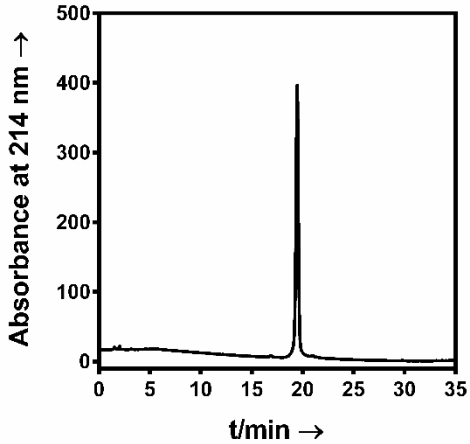

Peak #	Time (min)	Area	% Area
1	17.264	45.4	0.664
2	19.346	48.5	0.709
3	20.048	6572.9	96.176
4	21.705	167.5	2.451

Figure S5. Mass spectrometry and analytical HPLC characterization of a representative synthetic batch of $p3_{F20Y}$.

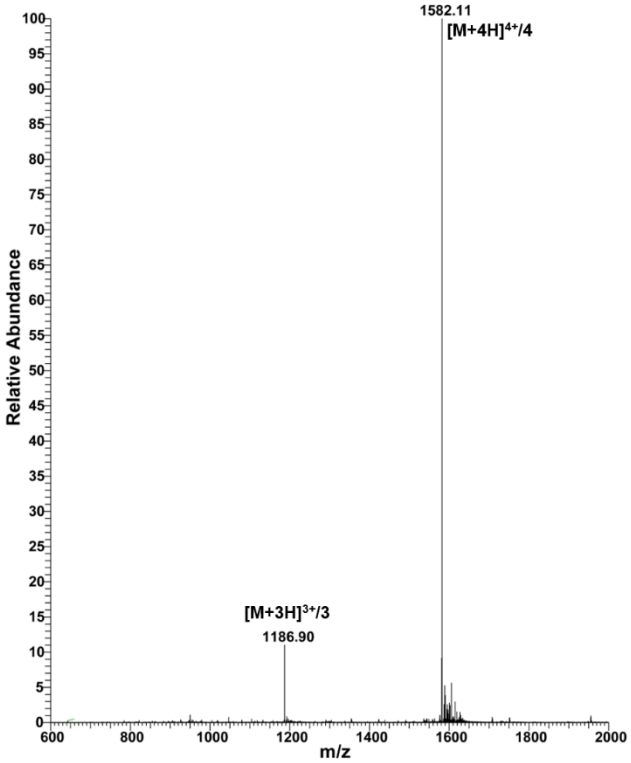

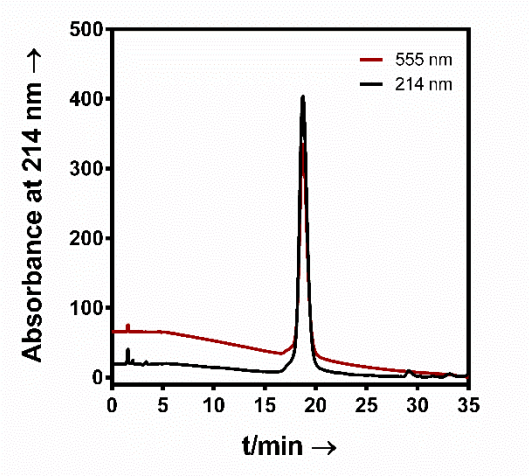

Peak #	Time (min)	Area	% Area
1	17.287	188	0.804
2	18.748	22674.3	96.960
3	29.136	334.1	1.429
4	33.154	188.9	0.808

Figure S6. Mass spectrometry and analytical HPLC characterization of a representative synthetic batch of TAMRA-labelled A$\beta_{1\text{-}40}$.

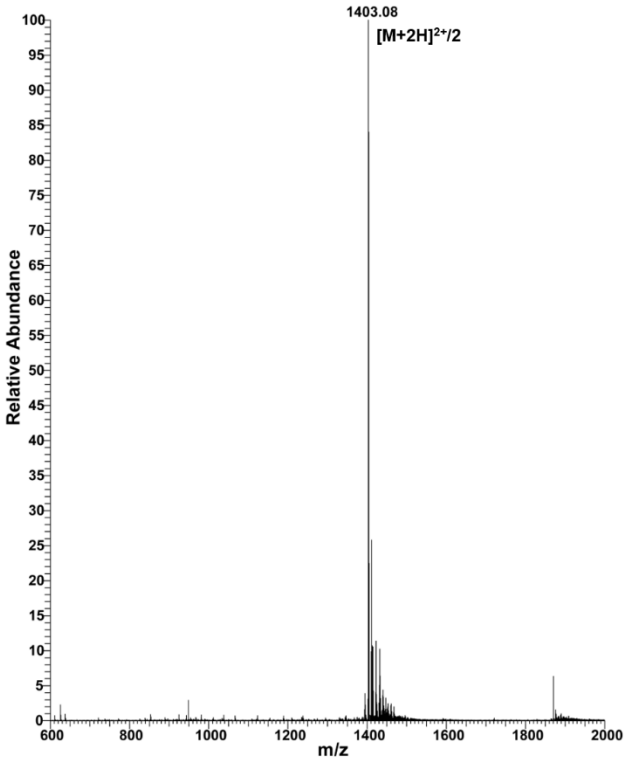

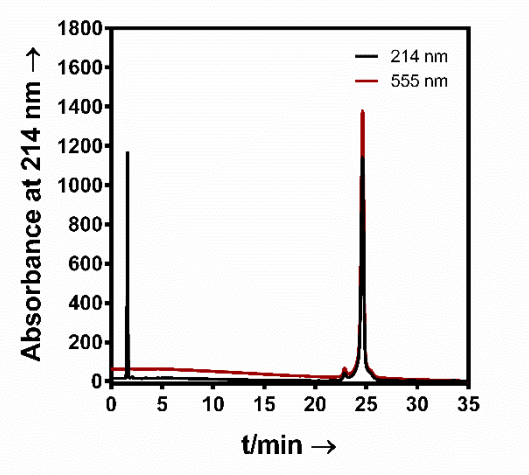

Peak #	Time (min)	Area	% Area
1	22.875	647.2	2.573
2	24.641	23772.7	94.517
3	25.231	732	2.910

Figure S7. Mass spectrometry and analytical HPLC characterization of a representative synthetic batch of TAMRA-labelled p3$_{17\text{-}40}$.

$A\beta_{1\text{-}40}$

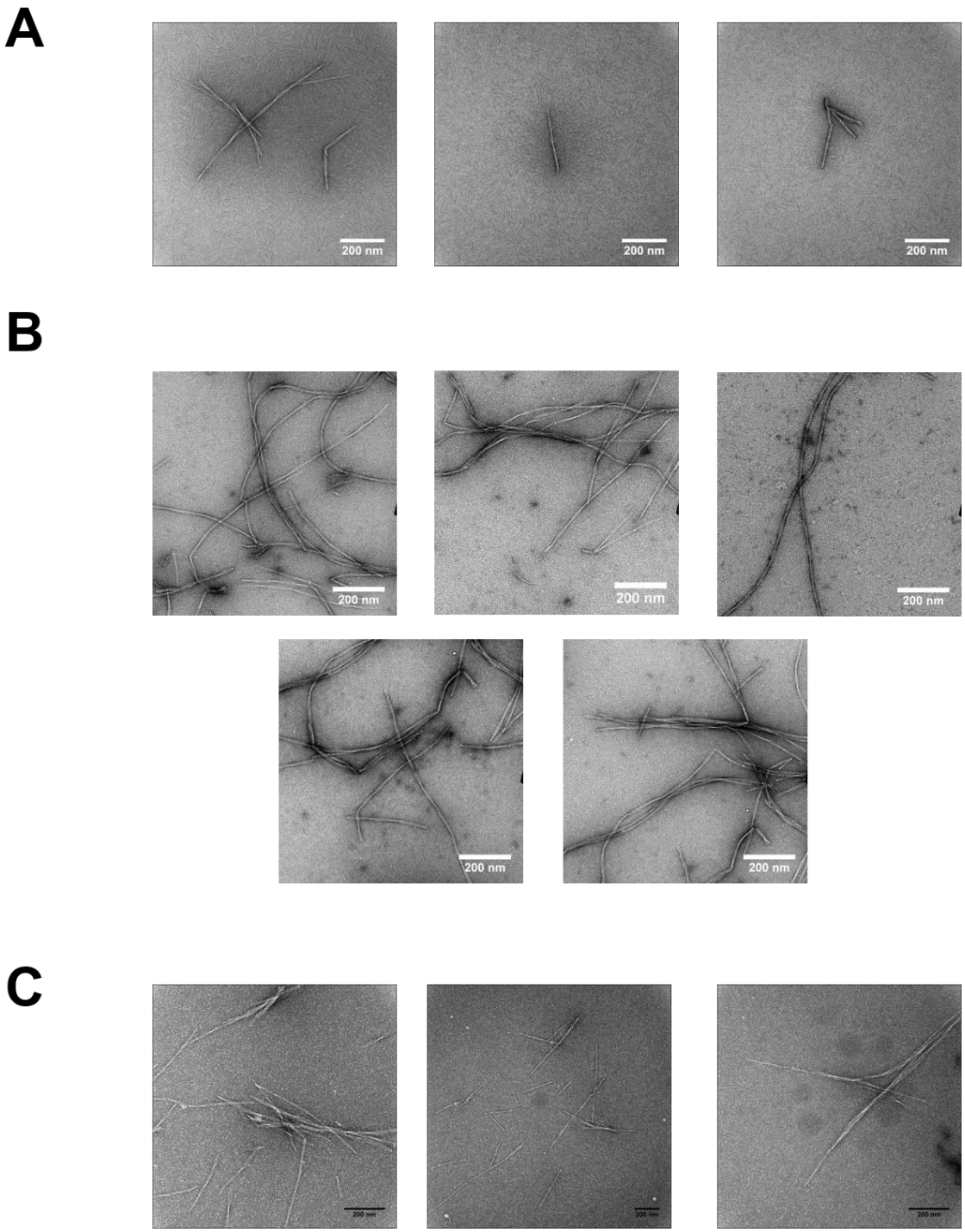

Figure S8. TEM images of $A\beta_{1\text{-}40}$ prepared A) quiescently (20 μM, 37 °C for 7 days) acquired at the University of California Santa Cruz Microscopy Center (JOEL 1230 Microscope), B) quiescently (20 μM, 37 °C for 7 days) acquired at the University of California Berkeley Electron Microscope Laboratory (Tecnai-12 Microscope), C) under agitation (20 μM, 37 °C for 24 hours with continuous shaking) acquired at the University of California Santa Cruz Microscopy Center (JOEL 1230 Microscope).

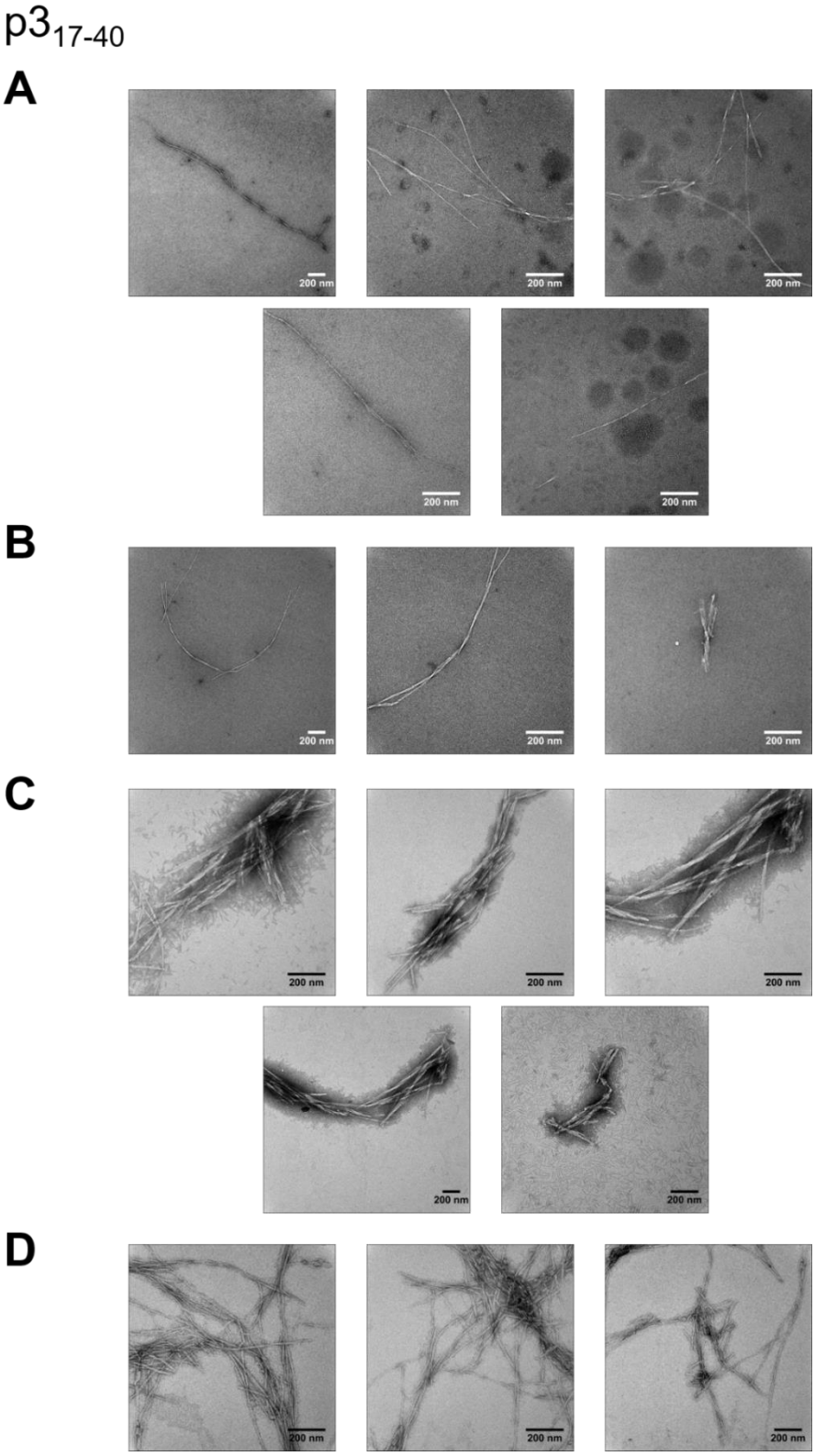

Figure S9. TEM images of p3$_{17-40}$ prepared A) quiescently (20 μM, 37 °C for 7 days), B) quiescently (40 μM, 37 C for 7 days), C) under agitation (20 μM, 37 °C for 24 hours with shaking every 5 minutes), D) TAMRA-labeled-p3$_{17-40}$ under agitation (20 μM, 37 °C for 24 hours with continuous shaking). A-D were acquired at the University of California Santa Cruz Microscopy Center (JOEL 1230 Microscope).

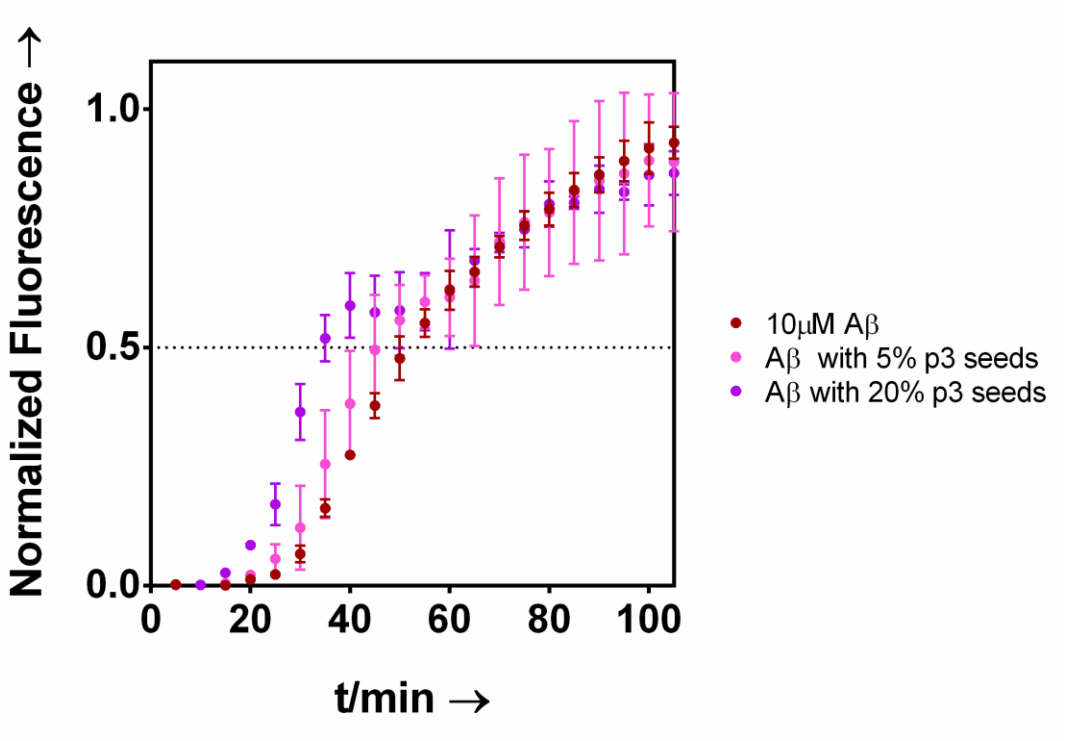

Figure S10. ThT- monitored aggregation kinetics of $A\beta_{1-40}$ alone, and amyloid beta with p3 fibrils added (at 5 or 20% of total concentration). p3 fibrils were formed at 37 °C under continuous shaking for 24 h, followed by centrifugation and washing x3.

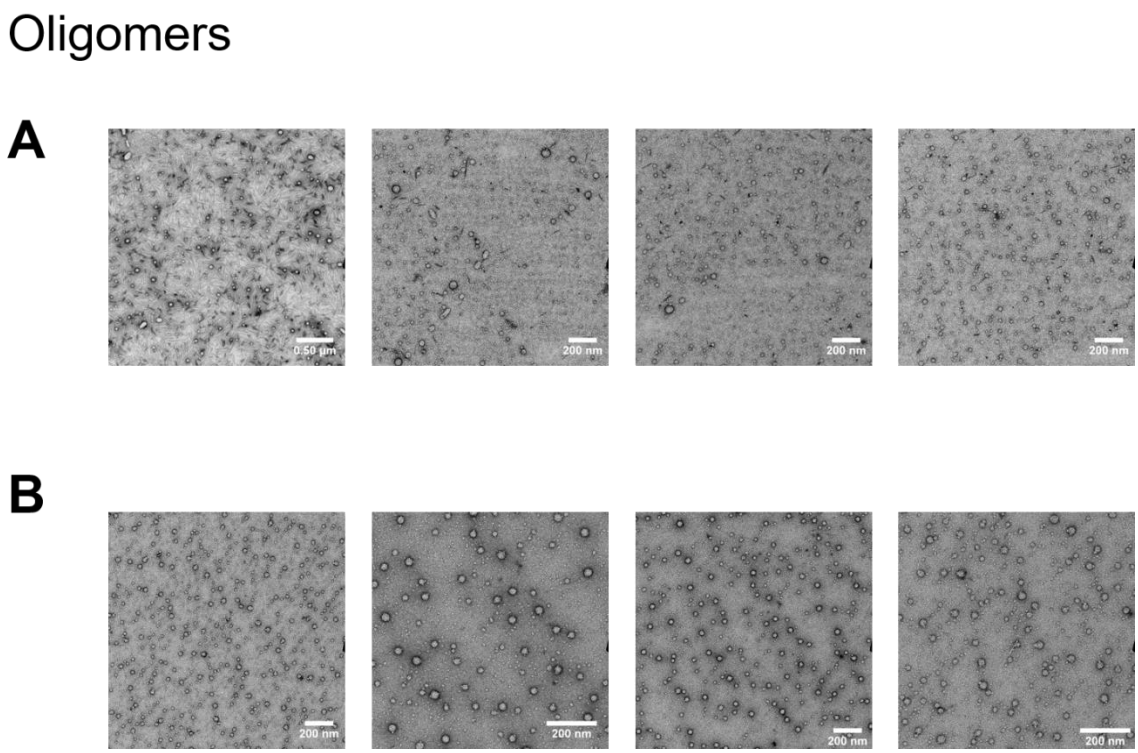

Figure S11. TEM images of kinetically trapped, intermediate oligomers of A) $A\beta_{1\text{-}40}$ (20 µM, 4 °C for 6 hours) and B) $p3_{17\text{-}40}$ (20 µM, 4 °C for 6 hours). These images were used to quantify the size distributions of spherical oligomers shown in Fig. 3C. Both A-B were acquired at the University of California Berkeley Electron Microscope Laboratory (Tecnai-12 Microscope).

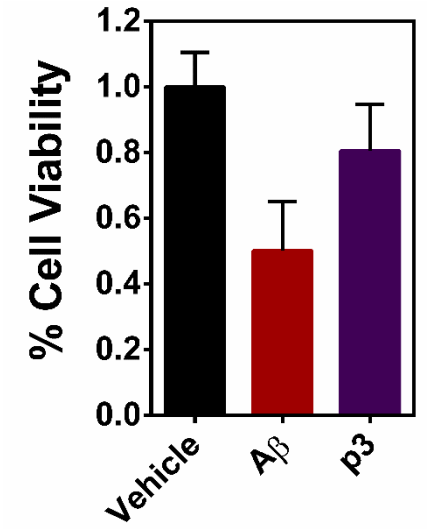

Figure S12. Cellular viability in SH-SY5Y cell lines following treatment with 50 µM oligomeric $A\beta_{1\text{-}40}$ or $p3_{17\text{-}40}$. Each sample, including controls, was incubated at 4 °C for 6 hours (consistent with method employed in Fig. 3 and S11, per published method by Ahmed *et. al.*[5])

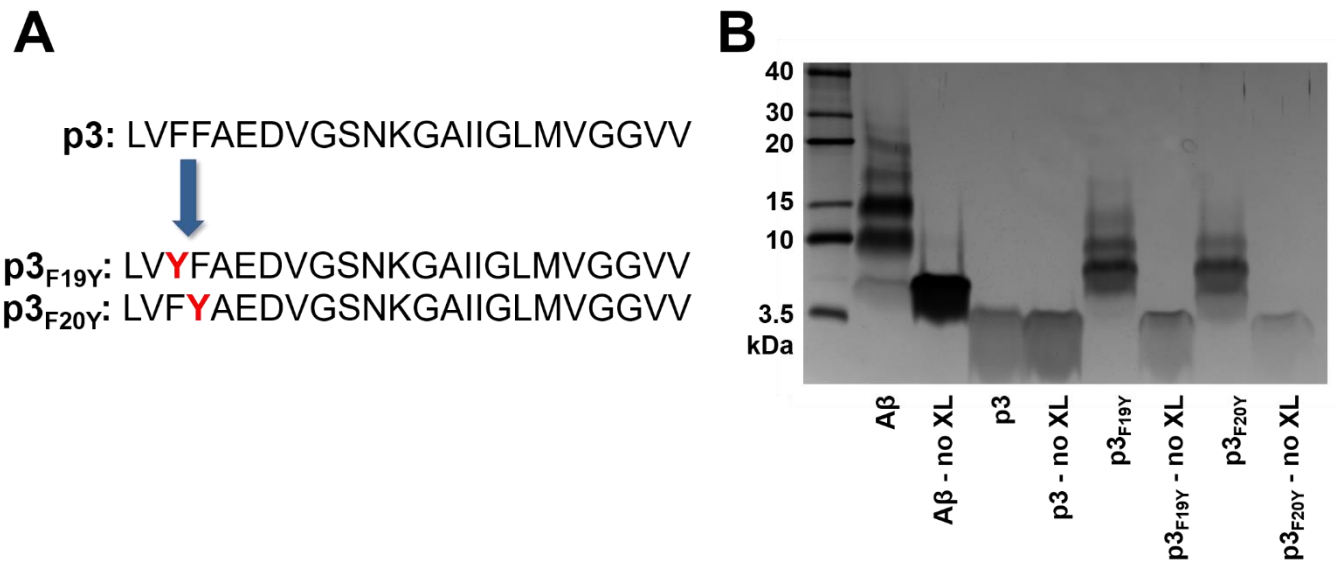

Figure S13. A) Sequence of p3 and 2 additional p3 peptides with Phe→ Tyr (F→ Y) substitutions at either the F19 or F20 position. B) SDS-PAGE gel of photo-induced crosslinked samples of Aβ, p3, $p3_{F19Y}$, and $p3_{F20Y}$. "No XL" denotes samples were not exposed to light.

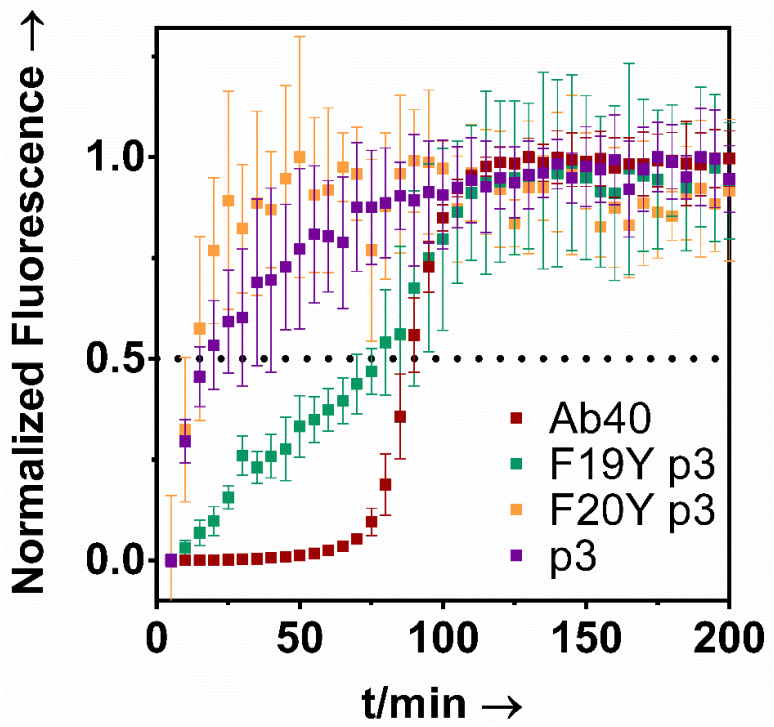

Figure S14. ThT- monitored aggregation kinetics of $A\beta_{1-40}$, $p3_{17-40}$, $p3_{F19Y}$, and $p3_{F20Y}$ (20 µM, 37 °C, with continuous shaking).

References

(1) Warner, C. J. A.; Dutta, S.; Foley, A. R.; Raskatov, J. A. Introduction of D-Glutamate at a Critical Residue of Aβ42 Stabilizes a Pre-Fibrillary Aggregate with Enhanced Toxicity. *Chem - A Eur J* **2016**, *22* (34), 11967–11970.

(2) AU - Warner, C. J. A.; AU - Dutta, S.; AU - Foley, A. R.; AU - Raskatov, J. A. A Tailored HPLC Purification Protocol That Yields High-Purity Amyloid Beta 42 and Amyloid Beta 40 Peptides, Capable of Oligomer Formation. *JoVE* **2017**, No. 121, e55482. https://doi.org/doi:10.3791/55482.

(3) Anthis, N. J.; Clore, G. M. Sequence-Specific Determination of Protein and Peptide Concentrations by Absorbance at 205 Nm. *Protein Sci* **2013**, *22* (6), 851–858. https://doi.org/10.1002/pro.2253.

(4) Nakka, P. P.; Li, K.; Forciniti, D. Effect of Differences in the Primary Structure of the A-Chain on the Aggregation of Insulin Fragments. *ACS OMEGA* **2018**, *3*, 9636–9647. https://doi.org/10.1021/acsomega.8b00500.

(5) Ahmed, M.; Davis, J.; Aucoin, D.; Sato, T.; Ahuja, S.; Aimoto, S.; Elliott, J. I.; Van Nostrand, W. E.; Smith, S. O. Structural Conversion of Neurotoxic Amyloid-Beta(1-42) Oligomers to Fibrils. *Nat Struct Mol Biol* **2010**, *17* (5), 561–567. https://doi.org/10.1038/nsmb.1799.

(6) Lalowski, M.; Golabek, A.; Lemere, C. A.; Selkoe, D. J.; Wisniewski, H. M.; Beavis, R. C.; Frangione, B.; Wisniewski, T. The "Nonamyloidogenic" P3 Fragment (Amyloid Beta 17-42) Is a Major Constituent of Down's Syndrome Cerebellar Preamyloid. *J Biol Chem* **1996**, *271* (52), 33623–33631. https://doi.org/10.1074/jbc.271.52.33623.

(7) Gowing, E.; Roher, A. E.; Woods, A. S.; Cotter, R. J.; Chaney, M.; Little, S. P.; Ball, M. J. Chemical Characterization of Abeta 17-42 Peptide, a Component of Diffuse Amyloid Deposits of Alzheimer Disease. *J Biol Chem* **1994**, *269* (15), 10987–10990.

(8) Näslund, J.; Schierhorn, A.; Hellman, U.; Lannfelt, L.; Roses, a D.; Tjernberg, L. O.; Silberring, J.; Gandy, S. E.; Winblad, B.; Greengard, P. Relative Abundance of Alzheimer A Beta Amyloid Peptide Variants in Alzheimer Disease and Normal Aging. *Proc Natl Acad Sci USA* **1994**, *91* (18), 8378–8382. https://doi.org/10.1073/pnas.91.18.8378.

(9) Saido, T. C.; Yamao-Harigaya, W.; Iwatsubo, T.; Kawashima, S. Amino- and Carboxyl-Terminal Heterogeneity of β-Amyloid Peptides Deposited in Human Brain. *Neurosci Lett* **1996**, *215* (3), 173–176. https://doi.org/10.1016/S0304-3940(96)12970-0.

(10) Higgins, L. S.; Murphy, G. M.; Forno, L. S.; Catalano, R.; Cordell, B. P3 Beta-Amyloid Peptide Has a Unique and Potentially Pathogenic Immunohistochemical Profile in Alzheimer's Disease Brain. *Am J Pathol* **1996**, *149* (2), 585–596.

(11) Abraham, J. D.; Prome, S.; Salvetat, N.; Rubrecht, L.; Cobo, S.; du Paty, E.; Galea, P.; Mathieu-Dupas, E.; Ranaldi, S.; Caillava, C.; Cremer, G. A.; Rieunuer, F.; Robert, P.; Molina, F.; Laune, D.; Checler, F.; Fareh, J. Cerebrospinal Aβ 11-x and 17-x Levels as Indicators of Mild Cognitive Impairment and Patients' Stratification in Alzheimer's Disease. *Transl Psychiatry* **2013**, *3* (e281), 1–8. https://doi.org/10.1038/tp.2013.58.

(12) Shi, J. M.; Zhang, L.; Liu, E. Q. Dissecting the Behaviour of β-Amyloid Peptide Variants during Oligomerization and Fibrillation. *J Pept Sci* **2017**, *23* (11), 810–817. https://doi.org/10.1002/psc.3028.

(13) Milton, N. G. N.; Harris, J. R. Polymorphism of Amyloid-β Fibrils and Its Effects on Human Erythrocyte Catalase Binding. *Micron* **2009**, *40* (8), 800–810. https://doi.org/10.1016/j.micron.2009.07.006.

(14) Vandersteen, A.; Hubin, E.; Sarroukh, R.; De Baets, G.; Schymkowitz, J.; Rousseau, F.; Subramaniam, V.; Raussens, V.; Wenschuh, H.; Wildemann, D.; Broersen, K. A Comparative Analysis of the Aggregation Behavior of Amyloid-β Peptide Variants. *FEBS Lett* **2012**, *586* (23), 4088–4093. https://doi.org/10.1016/j.febslet.2012.10.022.

(15) Naslund, J.; Jensen, M.; Tjernberg, L. O.; Thyberg, J.; Terenius, L.; Nordstedt, C. The Metabolic Pathway Generating P3, an Aβ Peptide Fragment, Is Probably Non-Amyloidogenic. *Biochem Biophys Res Commun* **1994**, *204* (2), 780–787. https://doi.org/10.1006/bbrc.1994.2527.

(16) Schmechel, A.; Zentgraf, H.; Scheuermann, S.; Fritz, G.; Reed, J.; Beyreuther, K.; Bayer, T. A.; Multhaup, G. Alzheimer β-Amyloid Homodimers Facilitate Aβ Fibrillization and the Generation of Conformational Antibodies*. *J Biol Chem* **2003**, *278* (37), 35317–35324. https://doi.org/10.1074/jbc.M303547200.

(17) Pike, C. J.; Overman, M. J.; Cotman, C. W. Amino-Terminal Deletions Enhance Aggregation of β-Amyloid Peptides in Vitro. *J Biol Chem* **1995**, *270* (41), 23895–23899.

(18) Zheng, J.; Jang, H.; Ma, B.; Tsai, C.-J.; Nussinov, R. Modeling the Alzheimer Aβ17-42 Fibril Architecture: Tight Intermolecular Sheet-Sheet Association and Intramolecular Hydrated Cavities. *Biophys J* **2007**, *93* (9), 3046–3057. https://doi.org/10.1529/biophysj.107.110700.

(19) Dulin, F.; Léveillé, F.; Ortega, J. B.; Mornon, J. P.; Buisson, A.; Callebaut, I.; Colloc'h, N. P3 Peptide, a Truncated Form of Aβ Devoid of Synaptotoxic Effect, Does Not Assemble into Soluble Oligomers. *FEBS Lett* **2008**, *582* (13), 1865–1870. https://doi.org/10.1016/j.febslet.2008.05.002.

(20) Streltsov, V. A.; Varghese, J. N.; Masters, C. L.; Nuttall, S. D. Crystal Structure of the Amyloid-β P3 Fragment Provides a Model for Oligomer Formation in Alzheimer's Disease. *J Neurosci* **2011**, *31* (4), 1419–1426. https://doi.org/10.1523/JNEUROSCI.4259-10.2011.

(21) Cheon, M.; Kang, M.; Chang, I. Polymorphism of Fibrillar Structures Depending on the Size of Assembled Aβ17-42 Peptides. *Sci Rep* **2016**, *6* (November), 38196. https://doi.org/10.1038/srep38196.

(22) Cheon, M.; Hall, C. K.; Chang, I. Structural Conversion of Aβ17–42 Peptides from Disordered Oligomers to U-Shape Protofilaments via Multiple Kinetic Pathways. *PLoS Comput Biol* **2015**, *11* (5), 1–23. https://doi.org/10.1371/journal.pcbi.1004258.

(23) Miller, Y.; Ma, B.; Nussinov, R. Polymorphism of Alzheimer's Aβ17-42 (P3) Oligomers: The Importance of the Turn Location and Its Conformation. *Biophys J* **2009**, *97* (4), 1168–1177. https://doi.org/10.1016/j.bpj.2009.05.042.

(24) Liu, R.; McAllister, C.; Lyubchenko, Y.; Sierks, M. R. Residues 17-20 and 30-35 of β-Amyloid Play Critical Roles in Aggregation. *J Neurosci Res* **2004**, *75* (2), 162–171. https://doi.org/10.1002/jnr.10859.

(25) Wei, W.; Norton, D. D.; Wang, X.; Kusiak, J. W. Aβ 17-42 in Alzheimer's Disease Activates JNK and Caspase-8 Leading to Neuronal Apoptosis. *Brain* **2002**, *125*, 2036–2043. https://doi.org/10.1093/brain/awf205.

(26) Jang, H.; Arce, F. T.; Ramachandran, S.; Capone, R.; Azimova, R.; Kagan, B. L.; Nussinov, R.; Lal, R. Truncated β-Amyloid Peptide Channels Provide an Alternative Mechanism for Alzheimer's Disease and Down Syndrome. *Proc Natl Acad Sci* **2010**, *107* (14), 6538–6543. https://doi.org/10.1073/pnas.0914251107.

(27) Walsh, D. M.; Klyubin, I.; Fadeeva, J. V.; Cullen, W. K.; Anwyl, R.; Wolfe, M. S.; Rowan, M. J.; Selkoe, D. J. Naturally Secreted Oligomers of Amyloid-β Protein Potently Inhibit Hippocampal Long-Term Potentiation in Vivo. *Nature* **2002**, *416* (6880), 535–539. https://doi.org/10.1038/416535a.

(28) Szczepanik, A. M.; Rampe, D.; Ringheim, G. E. Amyloid-Beta Peptide Fragments P3 and P4 Induce pro-Inflammatory Cytokine and Chemokine Production in Vitro and in Vivo. *J Neurochem* **2001**, *77* (1), 304–317. https://doi.org/10.1046/j.1471-4159.2001.00240.x.